Electrolyte Design Enabling Practical Lithium−Sulfur Batteries via Interfacial Manipulation and Inhibited Polysulfide Dissolution

Yilong Lin[a,], Zexian Zhang[b], Junru Wu[c], Jiayi Wang[a], Yuqing Jia[a], Xiaojin Jin[a], Feng Liu[a], Sheng Huang[b,*], Yanwu Chen[a], Yuezhong Meng[b,*]*

[a] College of Light Chemical Industry and Materials Engineering, Shunde Polytechnic, Foshan, 528333, China

[b] The Key Laboratory of Low-carbon Chemistry & Energy Conservation of Guangdong Province, State Key Laboratory of Optoelectronic Materials and Technologies, School of Materials Science and Engineering, Sun Yat-sen University, Guangzhou 510275, China

[c] Institute of Materials Research, Tsinghua Shenzhen International Graduate School, Tsinghua University, Shenzhen 518055, China

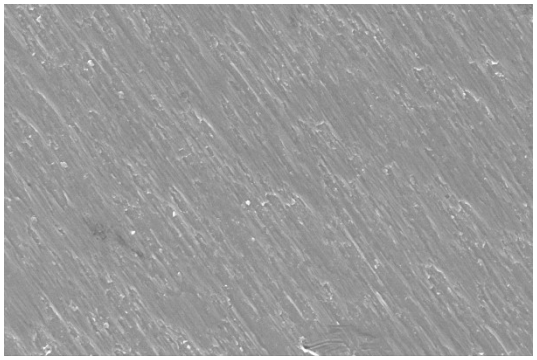

Figure S1. Surface SEM of fresh Cu electrode.

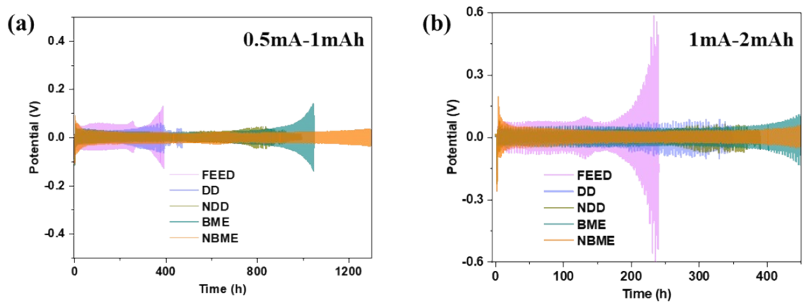

Figure S2. Cycling performances of Li/Li symmetric cells using different electrolytes at a current density and charge/discharge capacity of 0.5 mA cm^{-2}/1 mA h cm^{-2} (a) and 1 mA cm^{-2}/2 mA h cm^{-2} (b).

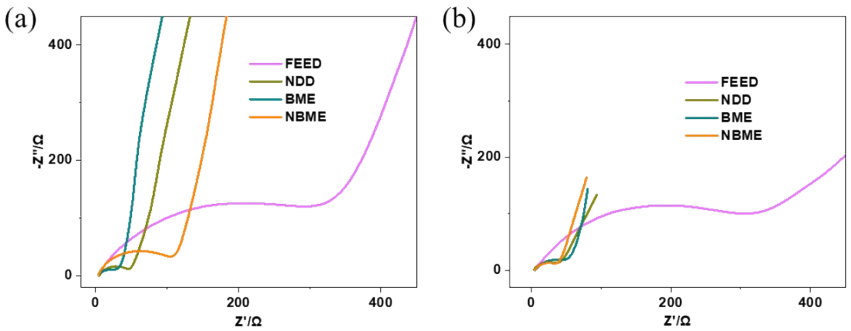

Figure S3. EIS analyses of Li/Cu cells after 10 (a) and 50 (b) cycles with different electrolytes.

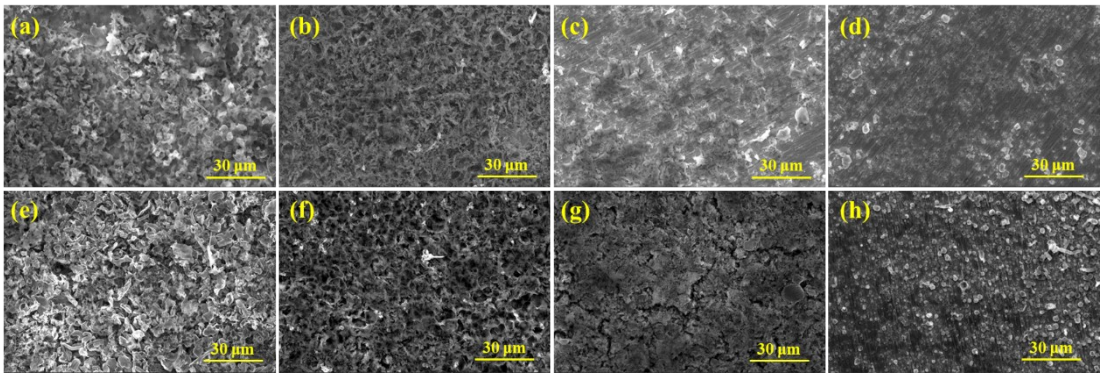

Figure S4. Surface SEM images of Cu anodes after 10 (a-d) and 50 (e-h) cycles in FEED (a,e), NDD (b,f), BME (c,g), NBME (d,h).

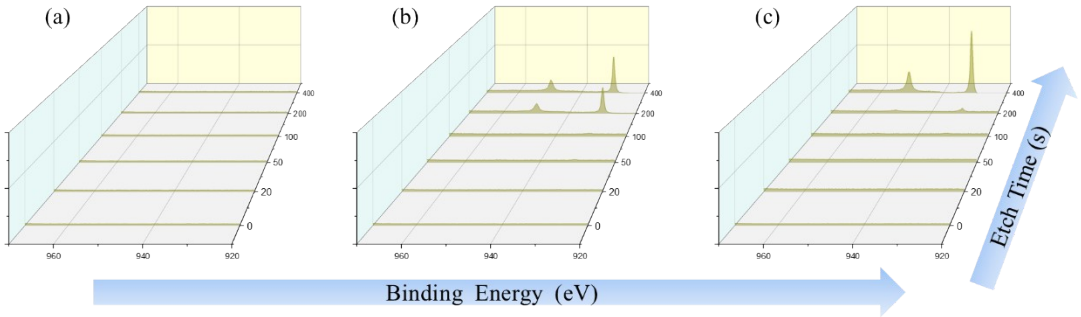

Figure S5. Cu 2*p* XPS in-depth spectra of the SEI layers formed on Cu anode using NDD (a), BME (b), NBME (c) electrolytes at different sputtering time.

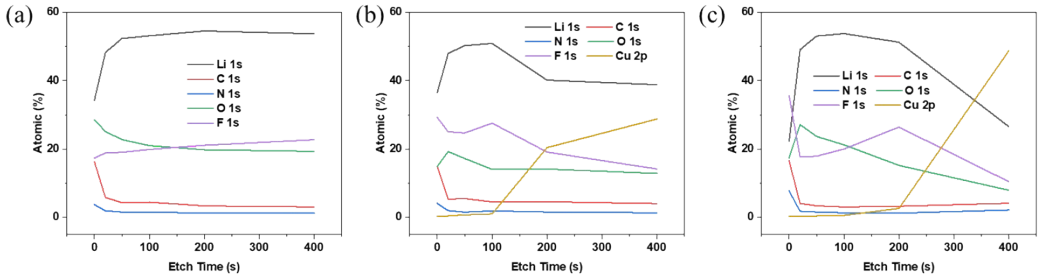

Figure S6. Quantified atomic concentrations of the detected elements on the SEI films on Li anode cycling in NDD (a), BME (b), NBME (c) electrolytes at different sputtering time.

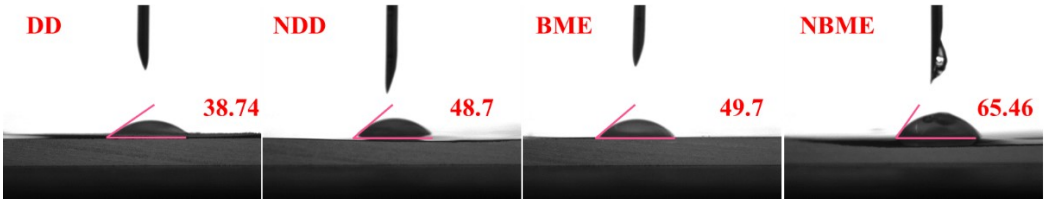

Figure S7. Digital photos of the contact angles between different electrolytes with the separator.

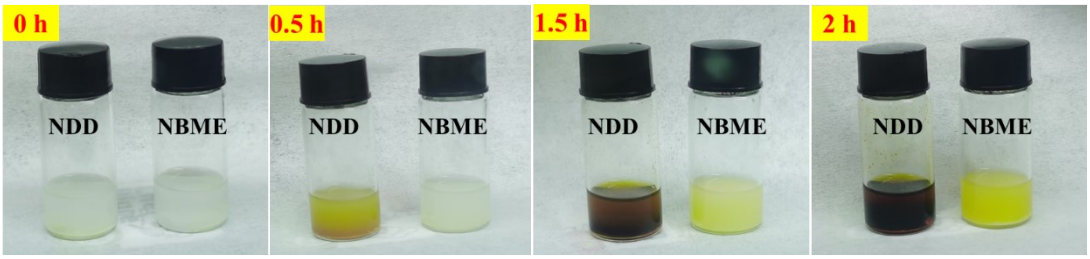

Figure S8. Polysulfide solubility test in NDD and BME electrolyte: Photo of NDD and BME electrolyte adding 0.5 M S_8 and 0.1 M Li_2S.

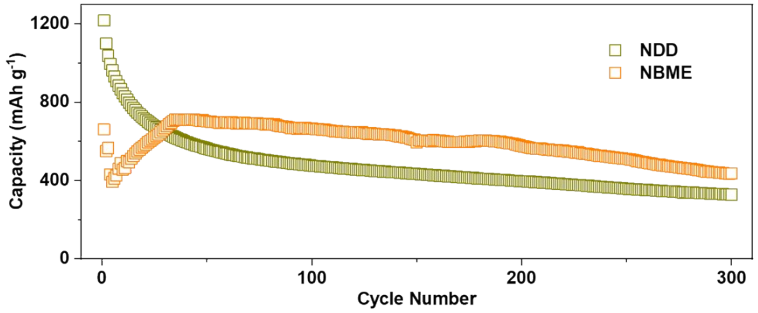

Figure S9. Cycling performance of Li–S coin cells with NDD and NBME electrolyte at 0.1 C.

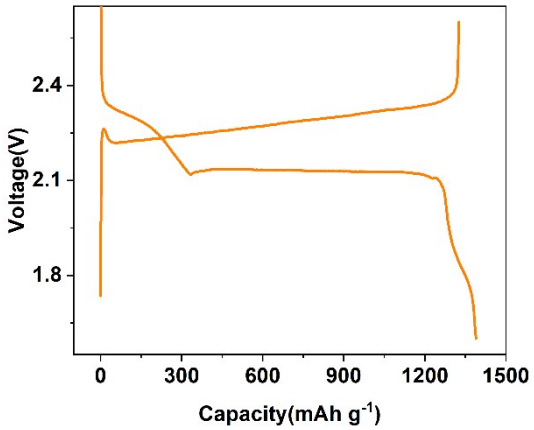

Figure S10. Initial discharge/charge curves of the Li/S cells with 5 mg cm^{-2} cathode and NBME electrolyte at 0.02 C.

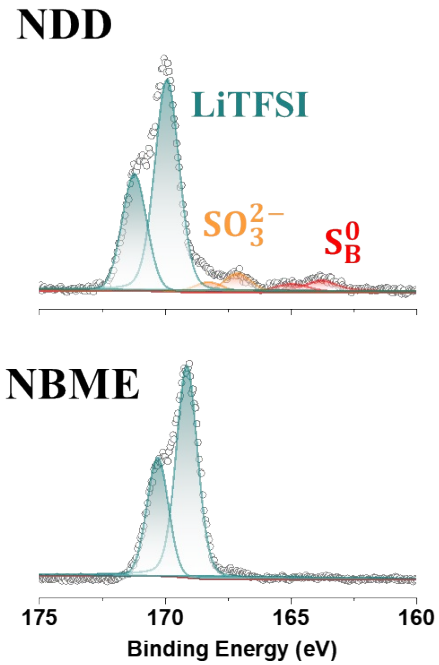

Figure S11. S spectra of cycled Li anodes from Li/S cells with NDD and NBME electrolyte.

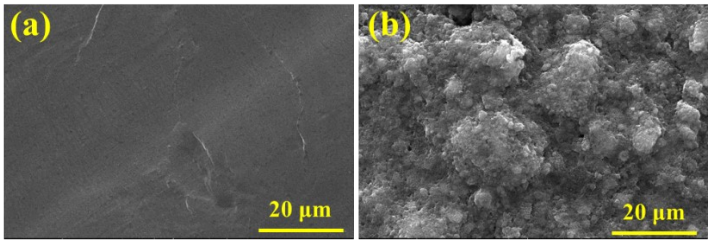

Figure S12. Surface SEM of fresh Li (a) and S (b) electrodes.

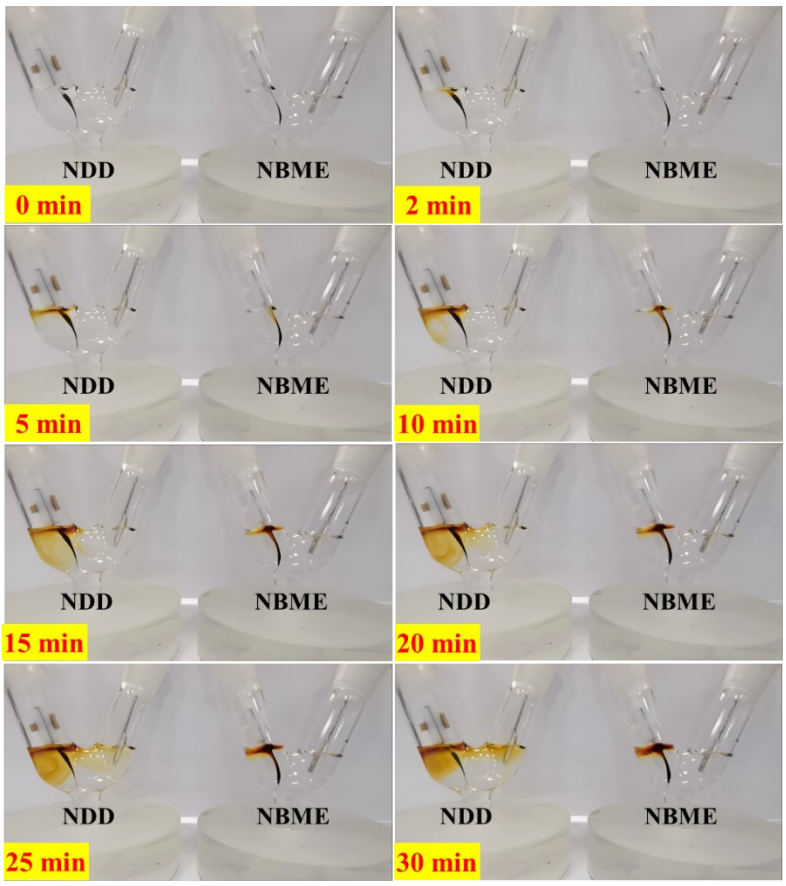

Figure S13. *Operando* visual V-type Li/S cell with NDD and NBME electrolyte during the discharing process.

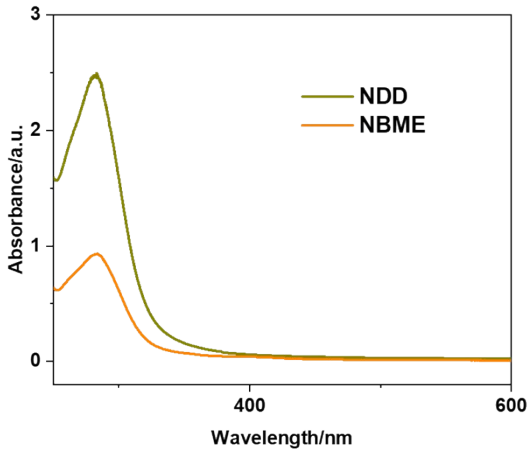

Figure S14. UV–vis absorption spectra of LiPS-containing DD electrolyte through immersing the cycled S cathode from the pouch cell with different electrolyte.

The cycled S cathodes from the pouch cells with NDD and NBME electrolytes were immersed in fresh DD electrolyte for 3 day. UV–vis absorption spectra of the LiPS-containing DD electrolyte with 50 times dilution display that a weaker LiPS signal was found in the cycled cathode with NBME than NDD electrolyte, demonstrating the less LiPS dissolution was formed in the cells with NBME during discharge/charge process.

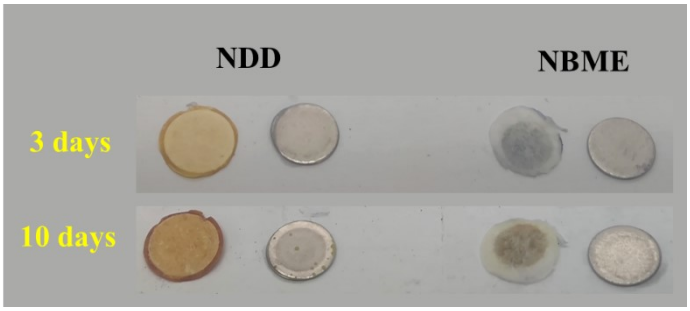

Figure S15. Photos of cycled glass fiber separators and Li anodes from Li/S coin cells after 3 and 10 days shelf time.

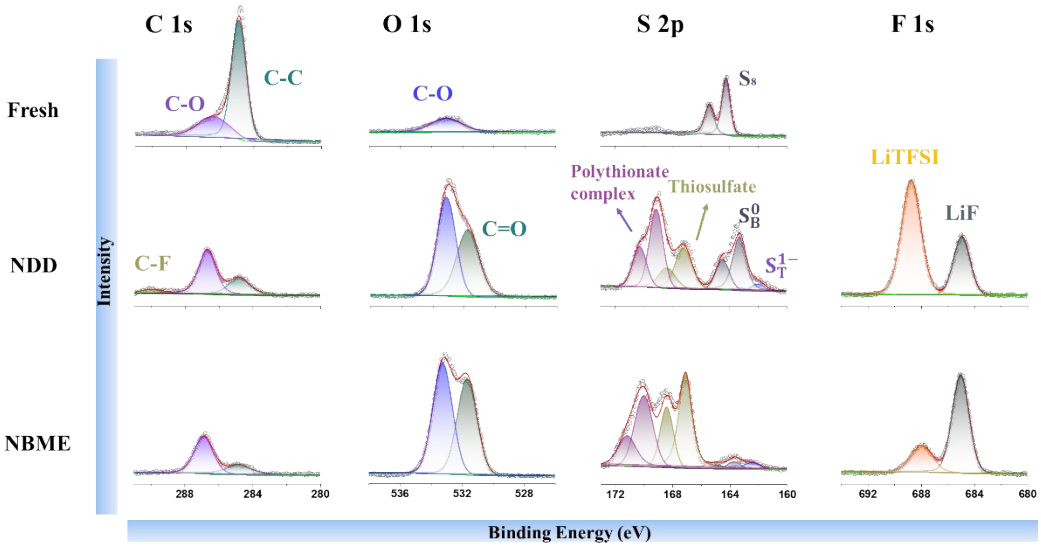

Figure S16. XPS spectra of fresh and cycled S cathodes from Li/S cells with NDD and NBME electrolyte.

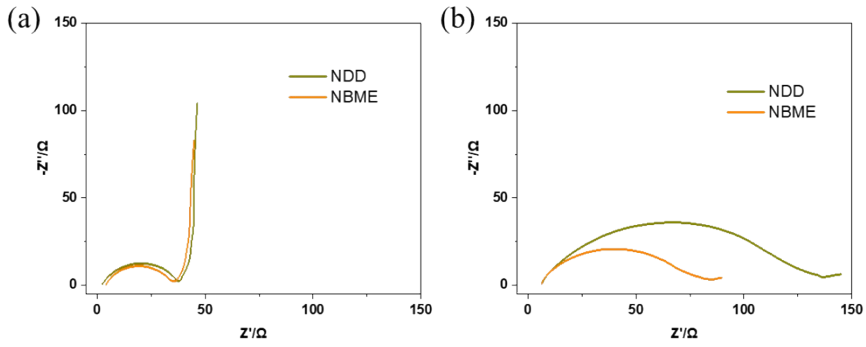

Figure S17. EIS analyses of Li/S cells before cycling (a) and after 10 cycles (b) with different electrolytes.

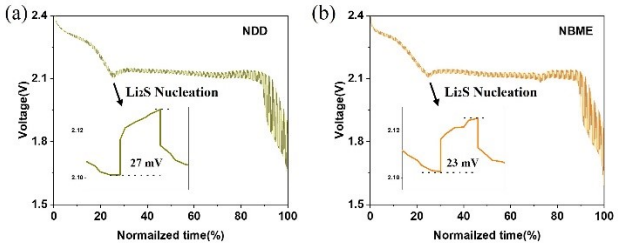

Figure S18. GITT voltage distribution for cells with NDD (a) and NBME (b) electrolyte.

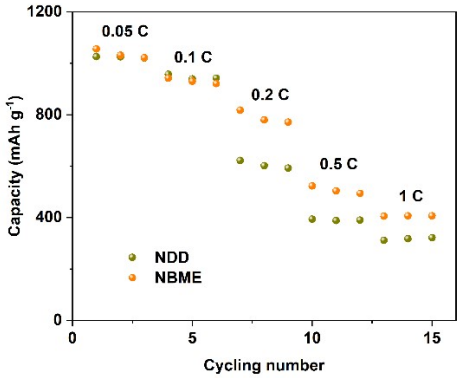

Figure S19. Rate capability for cells with NDD (a) and NBME (b) electrolyte after full activation during the formation process.

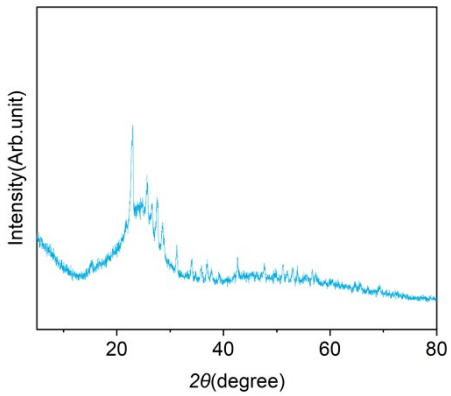

Figure S20. XRD pattern of S/KB composite.

Table S1 Comparison of Ah-level pouch cell performance of our work with previously reported work.

Tech.	Cycle number	Capacity retention (Rate, C)	Areal loading, mg/cm^2	E/S ratios, $\mu l\ mg^{-1}$	Ref.
Failure analysis	100	26%	4.43	3	Energy Storage Mater. 6, 18-25 (2017)
Electrolyte	40	77%	1.5	2.97	J. Electrochem. Soc. 164, A3766-A3771 (2017)
Separator	39	>90%	3.9	3.3	Matter 1, 1047-1060 (2019)

Failure analysis	40	33.5%	6	3	Energy Technol. 7, 1900111 (2019)
Cathode	40	93%	5.5	NA	Electrochim. Acta 356, 136815 (2020)
Electrolyte	26	84.2%	6.5	3.5	J. Am. Chem. Soc. 143, 11063-11071 (2021)
Cathode	30	88%	4.9	4	Adv. Mater. 33, 2007298 (2021)
Anode	25	77%	6.7	3.5	Angew. Chem. Int. Ed. e202204776 (2022)
Electrolyte	50	68%	2.78	4.5	Small 20, 2311850 (2024)
Cathode	70	65.7%	6.8	NA	ACS Appl. Mater. Interfaces 16, 35123 (2024)
Electrolyte	40	~88%	5	3.2	ACS Appl. Energy Mater. 7, 2210 (2024)
Electrolyte	60	70%	3	4	**This work**

Table S2 Density and viscosity of different electrolytes.

	DD	NDD	BME	NBME
Density (g/ml)		1.116		1.134
Viscosity (mPa·s)	44.716	76.517	99.157	118.33